Transit Met Chem (2017) 42:219–228
DOI 10.1007/s11243-017-0125-0

# Synthesis, characterization, and cytotoxicity of Pt(IV) complexes containing 1,10-phenanthroline and 2,2′-bipyridine and diaminocyclohexane ligands

**Xiaowei Zhao[1] · Yamei Zhang[1] · Xiaonan Hou[1] · Jianhong Shi[2] · Shigang Shen[1] · Shuying Huo[1]**

Received: 5 December 2016 / Accepted: 31 January 2017 / Published online: 22 February 2017


**Abstract** Four platinum(IV) complexes containing intercalating ligands [1,10-phenanthroline (phen) and 2,2′-bipyridine (bpy)] and ancillary ligands [(*1S,2S*)-diaminocyclohexane (*SS*-DACH) and (*1R,2R*)-diaminocyclohexane (*RR*-DACH)] were synthesized and characterized by $^{1}$H nuclear magnetic resonance, electrospray ionization mass spectrometry, X-ray crystal structure analysis, elemental analysis, ultraviolet absorption spectroscopy, circular dichroism spectroscopy, and electrochemical analysis. The reactions between [Pt(phen)(*SS*-DACH)$Cl_2$]$^{2+}$ and glutathione and Ac-CPFC-$NH_2$ were investigated by high-performance liquid chromatography. [Pt(phen)(*SS*-DACH)$Cl_2$]$^{2+}$ was reduced to its corresponding Pt(II) complex [Pt(phen)(*SS*-DACH)]$^{2+}$, while glutathione and Ac-CPFC-$NH_2$ were oxidized to glutathione-disulfide and a peptide containing an intramolecular disulfide bond, respectively. The cytotoxicities of the Pt(IV) complexes against a human non-small cell lung cancer cell line (A549) and the corresponding cisplatin-resistant cell line (A549cisR) were evaluated. These Pt(IV) complexes showed a higher activity toward A549 and A549cisR than did cisplatin. Also, the cytotoxicities of the Pt(IV) complexes were higher for A549cisR than for A549 cells. Moreover, the cytotoxicities of the (*SS*-DACH)-liganded platinum complexes were higher than those of the (*RR*-DACH)-liganded platinum complexes in either A549 or A549cisR cells. Phen-liganded platinum complexes were more cytotoxic than the bpy-liganded platinum complexes. The cytotoxicities of these Pt(IV) complexes had no correlation with reduction potentials.

## Introduction

Cisplatin and carboplatin have been used widely as drugs to treat a range of tumors. However, these drugs have some drawbacks, such as toxicity and tumor resistance, which have led researchers to design and investigate other types of platinum-based molecules as potential anticancer agents [1–5]. To this end, platinum(II) intercalators and platinum(IV) complexes, as new types of Pt-based drugs, have been developed for cancer therapy [6–11].

Recently, Aldrich-Wright and co-workers developed many Pt(II) intercalators, some of which were more biologically active than cisplatin in many cancer cell lines. Non-covalent binding to DNA is considered to play an important role in the cytotoxicity of the complexes [12–15]. The molecular formula of a general Pt(II) intercalator is [Pt(L)(A)]$^{2+}$, where L is the intercalating ligand, such as 1,10-phenanthroline (phen) and 2,2′-bipyridine (bpy), and A is the ancillary ligand, such as (*1S,2S*)-diaminocyclohexane (*SS*-DACH) and (*1R,2R*)-diaminocyclohexane (*RR*-

**Electronic supplementary material** The online version of this article (doi:10.1007/s11243-017-0125-0) contains supplementary material, which is available to authorized users.

✉ Jianhong Shi
shijianhong@hbu.edu.cn

✉ Shigang Shen
shensg@hbu.edu.cn

✉ Shuying Huo
shuyinghuo@126.com

[1] College of Chemistry and Environmental Science, Key Laboratory of Analytical Science and Technology of Hebei Province, and MOE Key Laboratory of Medicinal Chemistry and Molecular Diagnostics, Hebei University, Baoding 071002, Hebei Province, People's Republic of China

[2] Affiliated Hospital of Hebei University, Baoding 071000, Hebei Province, People's Republic of China

DACH). Changing L or A influences the complexes' biological activities. For example, methylated-phen as an intercalating ligand of the complex resulted in higher activity in cancer cells compared with that of the Pt(II) complex containing the phen ligand. By contrast, the stereo configuration of the ancillary ligand also influences the cytotoxicity of a platinum complex [14]. Moreover, the cytotoxicities of Pt(II) intercalators decreased with the increasing of concentration of glutathione, because glutathione degrades the complexes [16].

As an alternative, platinum(IV) complexes with anticancer activity have been developed for decades. Until now, none of the Pt(IV) compounds have been approved for clinical use; however, the advantages of Pt(IV) complexes, such as kinetic substitution inertness, oral administration, and higher accumulation in target cancer cells, have prompted researchers to develop these complexes [6, 8, 9, 17, 18]. Pt(IV) complexes are considered as prodrugs, because the complexes are activated by reduction to their Pt(II) species in cancer cells. Some small biological molecules, such as glutathione and ascorbic acid, have been accepted as reductants to reduce Pt(IV) complexes to their Pt(II) counterparts [19–25]. By contrast, Gibson and co-workers [26] found that cellular components with MW > 3000 Da are the main reductants for Pt(IV) complexes. Therefore, large protein molecules, such as thioredoxins, might reduce the Pt(IV) complexes in vivo. The reduction of Pt(IV) complexes, such as $Pt(NH_3)Cl_4$ and *trans*-$[Pt(CN)_4Cl_2]^{2-}$, by 3,6-dioxa-1,8-octanedithiol, which is a model compound of the active sites of thioredoxins, was investigated in our previous work. Those studies demonstrated that 3,6-dioxa-1,8-octanedithiol could reduce Pt(IV) complexes to their Pt(II) counterparts [27–29].

In this work, four Pt(IV) complexes containing chiral ancillary ligands (*SS*-DACH and *RR*-DACH) and intercalating ligands (phen and bpy), and their Pt(II) analogs, were prepared and characterized. The cytotoxicities of the Pt(IV) complexes against a human non-small cell lung cancer cell line (A549) and the corresponding cisplatin-resistant cell line (A549cisR) were investigated. Furthermore, reduction of the Pt(IV) complexes by glutathione and the Ac-CPFC-$NH_2$ peptide (representing the active sites of thioredoxins) was studied in detail.

## Experimental section

### Materials

All chemicals were used as received without further treatment. (*1S,2S*)-diaminocyclohexane (*SS*-DACH), (*1R,2R*)-diaminocyclohexane (*RR*-DACH), L-glutathione (GSH), oxidized L-glutathione (GSSG), 1,10-phenanthroline (phen), 2,2′-bipyridine (bpy), trifluoroacetic acid (TFA), *N,N*-dimethylformamide (DMF), and $K_2PtCl_4$ were purchased from Tansole Regent Company (Shanghai, China). $KMnO_4$, concentrated HCl, diethyl ether, acetonitrile, and ethanol were purchased from Tianjin Chemical Reagent Company (Tianjin, China). Fmoc-protected amino acids, Fmoc-Rink-amide-Am resin, and *O*-(Benzotriazol-1-yl)-*N,N,N′,N′*-tetramethyluronium tetrafluoroborate (HBTU) were purchased from GL Biochem (Shanghai, China). Diisopropylethylamine (DIEA), piperidine, and triisopropylsilane were purchased from Sigma-Aldrich.

### Instrumentation

$^1$H nuclear magnetic resonance (NMR) spectra were recorded on a Bruker AVANCE III 600 MHz digital NMR spectrometer (Bruker Daltonics Inc., Billerica, MA, USA). $D_2O$ was used as the solvent, with the water residue signal as a reference. High-resolution mass spectra were recorded on a Bruker Apex Ultra electrospray mass spectrometer (Bruker Daltonics Inc.). Elemental analysis for C, H, and N was performed on an Elementor instrument (Vario Micro cube, Germany). X-ray crystallography data were collected on a Bruker-AXS SMART APEX2 CCD diffractometer (Bruker AXS.). Ultraviolet spectra were recorded with a TU-1900 spectrophotometer (Beijing Puxi, Inc., Beijing, China) using 1.00-cm quartz cells. Circular dichroism spectra were recorded on a MOS 500 Circular Dichroism spectrometer (Bio-Logic, France). Analyses of Pt(IV) complexes and peptides, and the reaction between Pt(IV) complexes and peptide and GSH, were performed on a LC-20AB high-performance liquid chromatography (HPLC) system (Shimadzu, Japan). The reduction potentials of the Pt(IV) complexes were determined using a CHI 600E Electrochemical Workstation (CH Instruments, Inc., Shanghai, China).

### Synthesis of $[Pt(L)(A)]Cl_2$

Pt(II) complexes of $Pt(L)Cl_2$ (L is Phen or bpy) were synthesized according to our previous study [29]. Generally, 1,10-phenanthroline (0.2 g) was dissolved in HCl solution (10 mM, 40 mL), and then, $K_2PtCl_4$ (0.4 g, 10 mL) was added. The mixture was heated at 100 °C for 2 h under stirring. The yellow solid products obtained were washed with water until the pH reached 7.0. The yellow solid products were suspended in 50 mL of water, and then, A ((*SS*-DACH) or (*RR*-DACH)) (0.5 mL) was added. The mixture was heated at 100 °C to produce a pale yellow solution. This was cooled down to room temperature and then filtered through a G4 sintered glass filter. The filtrate was concentrated to about 2 mL on a rotary evaporator

under reduced pressure. The concentrated solution was treated with a solution containing ethanol and diethyl ether (1:6 V/V), resulting in a pale yellow precipitate. This was filtered off, washed with the mixture of ethanol and diethyl ether, and dried under a vacuum.

### General method for the synthesis of $[Pt(L)(A)Cl_2]Cl_2$

Pt(IV) complexes $[Pt(phen)(A)Cl_2]Cl_2$ were synthesized according to a previous report, with slight modifications [15, 16]. Generally, $[Pt(phen)(A)]Cl_2$ was dissolved in an HCl solution (10 mL), and then, $Cl_2$ gas was bubbled through the solution. This generated pale yellow solid products. After bubbling for another hour, the pale yellow products were filtered off, washed with a mixture of ethanol and diethyl ether, and then dried under a vacuum. To synthesize $[Pt(bpy)(A)Cl_2]Cl_2$, $Cl_2$ gas was also used as the oxidant and bubbled through the solution of $Pt(bpy)(A)Cl_2$ obtained by dissolving $[Pt(bpy)(A)]Cl_2$ in HCl solution (5 mL) and then bubbled with $N_2$ for another hour. The obtained solution was treated with a solution containing ethanol and diethyl ether (1:6 V/V), resulting in a pale yellow precipitate. This was filtered off, washed with the mixture of ethanol and diethyl ether, and dried under a vacuum.

### Synthesis of Ac-CPFC-$NH_2$ peptide

Peptide Ac-CPFC-$NH_2$ was synthesized using a Focus XC solid phase peptide synthesizer using standard Fmoc methodology. Fmoc-Rink-amide-Am resin (0.66 mmol/g, 250 mg) was used to synthesize the peptides. The coupling reactions were carried out using 3 mL of amino acid (0.33 mM) in DMF, 3 mL of HBTU (0.33 M) in DMF, and 2 mL of DIEA (1.0 M) in DMF for 50 min. Fmoc deprotection was performed using a 20% piperidine DMF solution. A cleavage cocktail containing 4% phenol, 2% water, 2% triisopropylsilane, and 92% TFA was used to cleave the peptide from the resin. The peptide was obtained by lyophilization and stored at −20 °C. The purity of the peptide was determined by a gradient reverse-phase (RP)-HPLC equipped with a UV–Vis detector at 215 nm using a 250 mm × 4.6 mm $C_8$ column at a flow rate of 1.0 mL/min. The solvent system used was A (0.1% TFA in $H_2O$) and B (0.1% TFA in MeCN). The elution protocol for analytical HPLC started with 0% B, followed by a linear gradient to 100% B over 15 min, maintained at 100% B for 5 min, and returned to 0% B over 10 min. The injection volume was 10 μL. The peptide (2 mg) was dissolved in a pH 4.5 buffer solution (1 mL) and then loaded onto the HPLC machine immediately.

### Ultraviolet (UV) absorption spectroscopy and circular dichroism (CD) spectroscopy

The UV spectra of the Pt(IV) complexes were recorded in water containing 0.1 M KCl. The addition of KCl inhibited the hydrolysis of the Pt(IV) complex [30–32]. A TU-1950 UV–Vis spectrophotometer with a 1.00-cm quartz cell was used to record the spectra of Pt(IV) complexes at room temperature from 200 to 400 nm. The CD spectra of HCl solutions containing 0.5 mM Pt(IV) complexes were recorded. Spectra were measured between 190 and 400 nm at 25 °C.

### High-performance liquid chromatography

The HPLC chromatograms of Pt(IV) complexes and the reactions between Pt(IV) complexes and Ac-CPFC-$NH_2$ and GSH were recorded on a Shimadzu LC-20AB machine equipped with a UV–Vis detector using a 250 mm × 4.6 mm $C_8$ column at a flow rate of 1.0 mL/min. The solvent system used was A (0.1% TFA in $H_2O$) and B (0.1% TFA in MeCN). The elution protocol for analytical HPLC started with 5% B, followed by a linear gradient to 8% B over 20 min, continuing to 90% B over 15 min, and finally returned to 5% over 5 min.

### Reduction potential

Cyclic voltammetric (CV) measurements were taken on a CHI 600E electrochemical analyzer with a scan rate of 50 mV/s. The working electrode was a glassy carbon electrode, the reference electrode was a saturated calomel electrode, and the auxiliary electrode was a platinum wire. Pt(IV) complexes were dissolved in 0.1 M KCl solution to a final concentration of 1 mM. All solutions were bubbled with nitrogen for 10 min before the CV determination.

### X-ray crystal structure analysis

Single crystals of $[Pt(phen)(\mathit{RR}\text{-DACH})Cl_2]Cl_2$ and $[Pt(bpy)(\mathit{SS}\text{-DACH})Cl_2]Cl_2$ were obtained by diffusing acetonitrile into an HCl solution (0.1 M) containing about 50 mg of the Pt(IV) complexes at room temperature. Single-crystal X-ray diffraction data were collected using a Bruker-AXS SMART APEX2 CCD diffractometer (Mo $K_\alpha$, $\lambda = 0.71073$ Å). Indexing was performed using APEX2 (Difference Vectors method). Data integration and reduction were performed using SaintPlus. Absorption correction was performed using a multi-scan method implemented in SADABS. Space groups were determined using XPREP implemented in APEX2. Structures were solved using SHELXL-97 program [33]. CCDC 1494132

and 1494133 contain the supplementary crystallographic data for the Pt(IV) complexes.

### Reduction of [Pt(phen)(*SS*-DACH)$Cl_2$]$Cl_2$ by thiol-containing compounds

*trans*-[$PtCl_2$(phen)(*SS*-DACH)]$^{2+}$ (0.25 mM) was reacted with GSH (0.75 mM) and Ac-CPFC-$NH_2$ (0.75 mM) in water, or a 10 mM HCl solution for 5 min, and then, the mixtures were analyzed by HPLC. As references, GSH, GSSG, and Pt(II) complex [Pt(phen)(*SS*-DACH)]$^{2+}$ were also analyzed by HPLC. Ac-CPFC-$NH_2$ and its oxidation product were characterized by electrospray ionization mass spectrometry (ESI–MS) in the positive mode.

### In vitro cytotoxicity evaluation

In vitro cytotoxicity evaluations were carried out in the Affiliated Hospital of Hebei University. The cytotoxicities of the Pt(IV) complexes against A549 and A549cisR cells were investigated using a WST-8 (sodium 2-(2-methoxy-4-nitrophenyl)-3-(4-nitrophenyl)-5-(2,4-disulfophenyl)-2H-tetrazolium) assay with Cell Counting Kit-8 (CCK-8). Generally, a suspension of cells (100 μL, $3 \times 10^4$ $mL^{-1}$) was plated in a 96-well plate with culture medium and incubated for 24 h at 37 °C in a 5% $CO_2$ incubator. Pt(IV) complexes and their corresponding Pt(II) complexes were dissolved in water and diluted to appropriate concentrations. Cisplatin was dissolved in DMSO and diluted to appropriate concentrations. All solutions of the platinum complexes were prepared and used daily. Various concentrations of platinum complexes were added into the wells and then incubated for 48 h at 37 °C in a 5% $CO_2$ incubator. The CCK-8 solution (10 μL, 5 mg/mL) was then added into the wells. After incubation for 4 h, the absorbance was measured at 450 nm.

## Results and discussion

### Synthesis and characterization

Four platinum(IV) complexes, [Pt(phen)(*SS*-DACH)$Cl_2$]$Cl_2$, [Pt(phen)(*RR*-DACH)$Cl_2$]$Cl_2$, [Pt(bpy)(*SS*-DACH)$Cl_2$]$Cl_2$, [Pt(bpy)(*RR*-DACH)$Cl_2$]$Cl_2$, were synthesized by oxidation of their Pt(II) analogs by chlorine gas in an HCl solution at room temperature. The purities of the Pt(IV) complexes were investigated using HPLC. HPLC chromatograms of the Pt(IV) complexes are shown in Figs. S1–S4, and the purities are listed in Table 1. Elemental analysis results for the Pt(IV) complexes are listed in Table S1, which are close to the calculated values for C, H, and N. Resolution ESI-mass spectra shown in Figs. S5–S8, and the obtained isotopic patterns almost equal to the calculated for Pt(IV) complexes. $^1$H NMR results for the Pt(II) and Pt(IV) complexes (Table 2) were consistent with those of the earlier reports [15, 34]. Moreover, the Pt(IV) or Pt(II) complexes possessing the same intercalator ligand exhibited similar *J* couplings and peak assignments. By contrast, downfield shifts were found when the Pt(II) complexes were oxidized to the corresponding Pt(IV) species, as shown in Fig. 1, because of the greater electronegativity of the higher oxidation state platinum [35].

### UV and CD spectra

The UV spectra of the Pt(IV) complexes are shown in Figs. S9–S13, which show that the two Phen-liganded Pt(IV) complexes have very similar UV spectra: Two strong bands at 208 and 278 nm were observed. The corresponding molar extinction coefficients are listed in Table 1. Moreover, a shoulder around 223 nm, a shoulder around 270 nm, and a shoulder-like feature at about 303 nm were also observed in the spectra. By contrast, the UV absorption spectrum of the Pt(II) complex of [Pt(phen)(*SS*-DACH)]$Cl_2$ is shown in Fig. S13 in comparison with the spectrum of [Pt(phen)(*SS*-DACH)$Cl_2$]$Cl_2$. Similar strong bands at about 278 nm were observed. Another strong band at 227 nm, a shoulder-like feature at about 300 nm, and a weak structured band system between 320 and 370 nm were observed, which were consistent with an earlier report [10].

The two bpy-liganded Pt(IV) complexes also had similar UV spectra. Three strong bands at 215, 308, and 320 nm were observed in the spectra. The corresponding molar extinction coefficients are listed in Table 1. The UV spectra of their Pt(II) analogs have been reported in a previous study [34]. The UV spectra of the Pt(II) and

**Table 1** Reduction potential, high-performance liquid chromatography, and ultraviolet characterization data of Pt(IV) complexes

| Pt(IV) complexes | $E_p$/mV | Purities (HPLC) [%] | $t_R$ (min) | UV $\lambda_{max}$/nm (ε/$mol^{-1}$ L $cm^{-1}$) |
|---|---|---|---|---|
| [Pt(phen)(*SS*-DACH)$Cl_2$]$Cl_2$ | 98 | 96 | 14.924 | 208 ($6.56 \times 10^4$), 278 ($2.96 \times 10^4$) |
| [Pt(phen)(*RR*-DACH)$Cl_2$]$Cl_2$ | 101 | 99 | 14.657 | 208 ($6.45 \times 10^4$), 278 ($2.86 \times 10^4$) |
| [Pt(bpy)(*SS*-DACH)$Cl_2$]$Cl_2$ | 82 | 98 | 9.279 | 215 ($4.99 \times 10^4$), 308 ($1.25 \times 10^4$), 320 ($1.43 \times 10^4$) |
| [Pt(bpy)(*RR*-DACH)$Cl_2$]$Cl_2$ | 86 | 98 | 9.221 | 215 ($4.91 \times 10^4$), 308 ($1.20 \times 10^4$), 320 ($1.40 \times 10^4$) |

**Table 2** $^{1}$H nuclear magnetic resonance data of Pt(II) complexes and Pt(IV) complexes

| No | Pt(IV) complex | Structure of cationic form of Pt(IV) complex | $^{1}$H NMR (600 MHz, $D_2O$) |
|---|---|---|---|
| 1 | [Pt(phen)(*SS*-DACH)]$Cl_2$ | 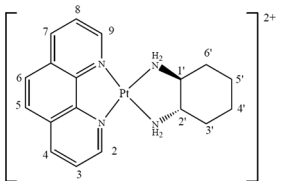 | $\delta$ = 1.20–1.28 (m, 2H; $CH_2$ (H4′, H5′)), 1.45–1.50 (m, 2H; $CH_2$ (H3′, H6′)), 1.65–1.67 (m, 2H; $CH_2$ (H4′, H5′)), 2.21–2.23 (m, 2H; $CH_2$ (H3′, H6′)), 2.69–2.75 (m, 2H; *CH* (H1′, H2′)), 7.99 (dd, $J$ = 6.0, 6.0 Hz, 2H; *CH* (H3, H8)), 8.10 (s, 2H; *CH* (H5, H6)), 8.86 (d, $J$ = 6.0 Hz, 2H; *CH* (H4, H7)), 8.89 (d, $J$ = 6.0 Hz, 2H; *CH* (H2, H9)). |
| 2 | [Pt(phen)(*RR*-DACH)]$Cl_2$ | 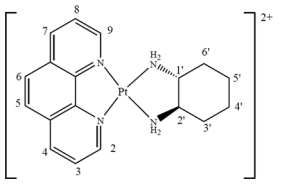 | $\delta$ = 1.19–1.27 (m, 2H; $CH_2$ (H4′, H5′)), 1.44–1.49 (m, 2H; $CH_2$ (H3′, H6′)), 1.64–1.65 (m, 2H; $CH_2$ (H4′, H5′)), 2.19–2.22 (m, 2H; $CH_2$ (H3′, H6′)), 2.68–2.73 (m, 2H; *CH* (H1′, H2′)), 7.97 (dd, $J$ = 6.0, 6.0 Hz, 2H; *CH* (H3, H8)), 8.09 (s, 2H; *CH* (H5, H6)), 8.85 (d, $J$ = 6.0 Hz, 2H; *CH* (H4, H7)), 8.88 (d, $J$ = 6.0 Hz, 2H; *CH* (H2, H9)). |
| 3 | [Pt(bpy)(*SS*-DACH)]$Cl_2$ | 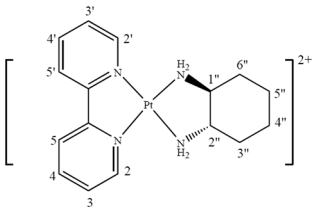 | $\delta$ = 1.15–1.22 (m, 2H; $CH_2$ (H4″, H5″)), 1.37–1.42 (m, 2H; $CH_2$ (H3″, H6″)), 1.60–1.62 (m, 2H; $CH_2$ (H4″, H5″)), 2.13–2.15 (m, 2H; $CH_2$ (H3″, H6″)), 2.58–2.63 (m, 2H; *CH* (H1″, H2″)), 7.68 (dt, $J$ = 2.4, 6.0 Hz, 2H; *CH* (H3, H3′)), 8.30–8.34 (m, 4H; *CH* (H4, H4′ and H5, H5′)), 8.51 (d, $J$ = 6.0 Hz, 2H; *CH* (H2, H2′)). |
| 4 | [Pt(bpy)(*RR*-DACH)]$Cl_2$ | 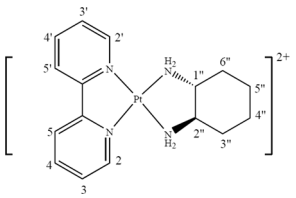 | $\delta$ = 1.13–1.21 (m, 2H; $CH_2$ (H4″, H5″)), 1.36–1.38 (m, 2H; $CH_2$ (H3″, H6″)), 1.58–1.60 (m, 2H; $CH_2$ (H4″, H5″)), 2.11–2.13 (m, 2H; $CH_2$ (H3″, H6″)), 2.58–2.60 (m, 2H; *CH* (H1″, H2″)), 7.66 (dt, $J$ = 3.6, 6.0 Hz, 2H; *CH* (H3, H3′)), 8.28–8.32 (m, 4H; *CH* (H4, H4′ and H5, H5′)), 8.49 (d, $J$ = 6.0 Hz, 2H; *CH* (H2, H2′)). |
| 5 | [Pt(bpy)(*SS*-DACH)$Cl_2$]$Cl_2$ | 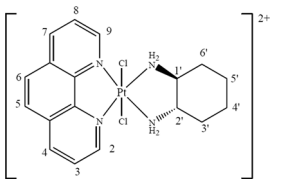 | $\delta$ = 1.26–1.33 (m, 2H; $CH_2$ (H4′, H5′)), 1.64–1.72 (m, 4H; $CH_2$ (H3′, H6′ and H4′, H5′)), 2.34–2.36 (m, 2H; $CH_2$ (H3′, H6′)), 3.31–3.37 (m, 2H; *CH* (H1′, H2′)), 8.26 (dd, $J$ = 6.0, 6.0 Hz, 2H; *CH* (H3, H8)), 8.32 (s, 2H; *CH* (H5, H6)), 9.05 (d, $J$ = 6.0 Hz, 2H; *CH* (H4, H7)), 9.08 (d, $J$ = 6.0 Hz, 2H; *CH* (H2, H9)). |
| 6 | [Pt(bpy)(*RR*-DACH)$Cl_2$]$Cl_2$ | 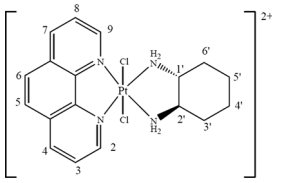 | $\delta$ = 1.26–1.33 (m, 2H; $CH_2$ (H4′, H5′)), 1.64–1.72 (m, 4H; $CH_2$ (H3′, H6′ and H4′, H5′)), 2.34–2.36 (m, 2H; $CH_2$ (H3′, H6′)), 3.31–3.37 (m, 2H; *CH* (H1′, H2′)), 8.26 (dd, $J$ = 6.0, 6.0 Hz, 2H; *CH* (H3, H8)), 8.33 (s, 2H; *CH* (H5, H6)), 9.05 (d, $J$ = 6.0 Hz, 2H; *CH* (H4, H7)), 9.08 (d, $J$ = 6.0 Hz, 2H; *CH* (H2, H9)). |
| 7 | [Pt(bpy)(*SS*-DACH)$Cl_2$]$Cl_2$ | 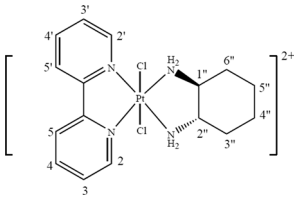 | $\delta$ = 1.22–1.29 (m, 2H; $CH_2$ (H4″, H5″)), 1.61–1.66 (m, 4H; $CH_2$ (H3′, H6′ and H4′, H5′)), 2.27–2.29 (m, 2H; $CH_2$ (H3″, H6″)), 3.21–3.27 (m, 2H; *CH* (H1″, H2″)), 7.98 (t, $J$ = 6.0, 12.0 Hz, 2H; *CH* (H3, H3′)), 8.49 (t, $J$ = 6.0, 12.0 Hz, 2H; *CH* (H4, H4′)), 8.66 (d, $J$ = 6.0 Hz, 2H; *CH* (H5, H5′)), 8.71 (d, $J$ = 6.0 Hz, 2H; *CH* (H2, H2′)). |
| 8 | [Pt(bpy)(*RR*-DACH)$Cl_2$]$Cl_2$ | 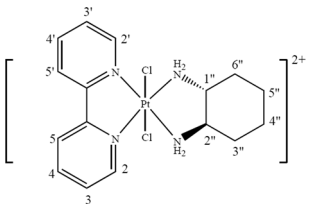 | $\delta$ = 1.20–1.28 (m, 2H; $CH_2$ (H4″, H5″)), 1.60–1.65 (m, 4H; $CH_2$ (H3′, H6′ and H4′, H5′)), 226–2.28 (m, 2H; $CH_2$ (H3″, H6″)), 3.20–3.25 (m, 2H; *CH* (H1″, H2″)), 7.97 (dt, $J$ = 1.8, 6.0 Hz, 2H; *CH* (H3, H3′)), 8.48 (dt, $J$ = 1.2, 6.0 Hz, 2H; *CH* (H4, H4′)), 8.65(d, $J$ = 12.0 Hz, 2H; *CH* (H5, H5′)), 8.69 (d, $J$ = 12.0 Hz, 2H; *CH* (H2, H2′)). |

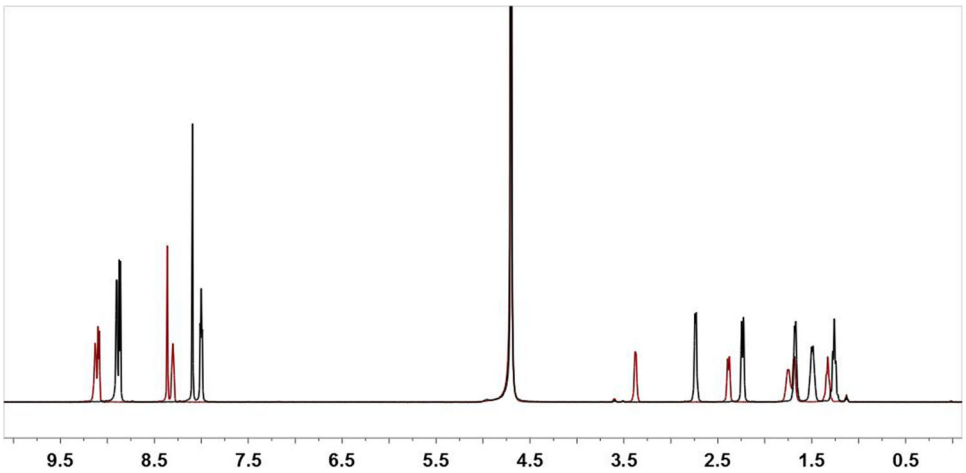


**Fig. 1** The 600 M $^1$H NMR in $D_2O$ of *red trans*-$[PtCl_2(phen)(RR\text{-DACH})]^{2+}$ and *black* $[Pt(phen)(RR\text{-DACH})]^{2+}$. (Color figure online)

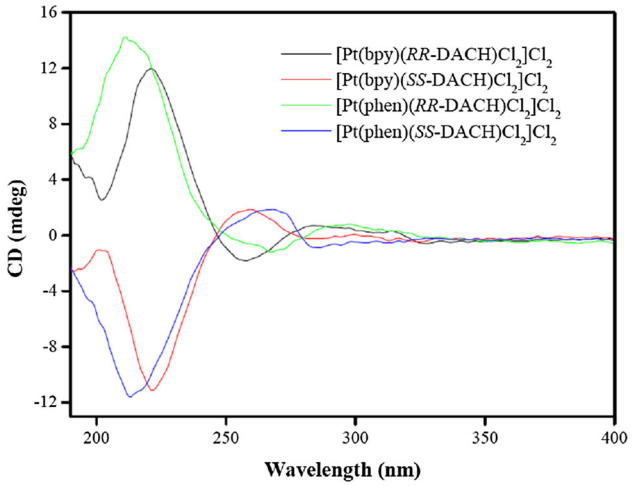


**Fig. 2** CD spectra of the Pt(IV) complexes

Pt(IV) complexes showed some similarities at wavelengths longer than 270 nm. However, the spectra were different below 270 nm: The Pt(II) complexes had a strong band at about 245 nm, while the Pt(IV) complex had a strong band at about 215 nm.

The chiralities of the Pt(IV) complexes in the present work were characterized by CD spectroscopy. The CD spectra (Fig. 2) showed that the chirality of each Pt(IV) complex was conserved during synthesis [10].

## Reduction potential

Cyclic voltammograms of the Pt(IV) complexes are shown in Fig. S14, and the values are listed in Table 1. The data showed that the conformation of the ancillary ligand (*RR*-DACH/*SS*-DACH) had no influence on the reduction potential of the Pt(IV) complexes. The reduction potential was slightly increased when the intercalating ligand changed from bpy to phen.

## X-ray crystal structures of the Pt(IV) complexes

Single crystal structures of $[Pt(phen)(RR\text{-DACH})Cl_2]Cl_2$ and $[Pt(bpy)(SS\text{-DACH})Cl_2]Cl_2$ were obtained by the slow diffusion of acetonitrile into an HCl solution containing the Pt(IV) complex at room temperature. Crystallographic parameters are listed in Table 3. The X-ray structures of the Pt(IV) complexes are shown in Fig. 3. The two Pt(IV) complexes have an octahedral coordination geometry around the Pt(IV) ion. The equatorial plane is occupied by nitrogen ligands, whereas the axial positions are occupied by two chloride ligands. Moreover, the DACH ligand is disorderly in the crystal structures of the Pt(IV) complexes, which is usually observed in other chiral DACH-liganded Pt(IV) complexes [10].

## Reduction of $[Pt(phen)(SS\text{-DACH})Cl_2]Cl_2$ by thiol-containing compounds

The purity of Ac-CPFC-$NH_2$ was analyzed by HPLC as 82% (Fig. S15). This peptide was characterized by ESI–MS in the positive mode $([M+H^+]^+$ *m/z* 510.18) and used without further purification. In the present work, reduction of $[Pt(phen)(SS\text{-DACH})Cl_2]Cl_2$ by GSH and Ac-CPFC-$NH_2$ was studied using HPLC. HPLC chromatograms of GSH, GSSG, $[Pt(phen)(SS\text{-DACH})]^{2+}$, *trans*-$[PtCl_2(phen)(SS\text{-DACH})]^{2+}$ and the reaction mixture of *trans*-$[PtCl_2(phen)(SS\text{-DACH})]^{2+}$ with glutathione are shown in Fig. 4. *trans*-$[PtCl_2(phen)(SS\text{-DACH})]^{2+}$ was reduced to $[Pt(phen)(SS\text{-DACH})]^{2+}$ by GSH, while the oxidation product of GSH was GSSG. HPLC chromatograms of $[Pt(phen)(SS\text{-DACH})]^{2+}$, *trans*-$[PtCl_2(phen)(SS\text{-DACH})]^{2+}$, Ac-CPFC-$NH_2$, and the reaction mixture of *trans*-$[PtCl_2(phen)(SS\text{-DACH})]^{2+}$ with Ac-CPFC-$NH_2$, are shown in Fig. 5. The products of the reaction between *trans*-$[PtCl_2(phen)(SS\text{-DACH})]^{2+}$ and Ac-CPFC-$NH_2$ are $[Pt(phen)(SS\text{-DACH})]^{2+}$ and the oxidized form of Ac-CPFC-$NH_2$, containing an intramolecular disulfide bond. The oxidized

**Table 3** Crystal data and structure refinement for [Pt(phen)(*RR*-DACH)$Cl_2$]$Cl_2$ and [Pt(bpy)(*SS*-DACH)$Cl_2$]$Cl_2$

| | [Pt(bpy)(*SS*-DACH)$Cl_2$]$Cl_2$ | [Pt(phen)(*RR*-DACH)$Cl_2$]$Cl_2$ |
|---|---|---|
| Formula | $C_{16}H_{22}Cl_4N_4Pt$ | $C_{18}H_{22}Cl_4N_4Pt$ |
| *Mr* | 607.27 | 631.29 |
| *T* (K) | 296(2) | 296(2) |
| Crystal system | Monoclinic | Monoclinic |
| Space group | *C*2/m | *P*21/c |
| *a* (Å) | 28.9620 (17) | 9.4168 (3) |
| *b* (Å) | 11.8737 (6) | 15.9236 (6) |
| *c* (Å) | 15.5581 (7) | 29.4696 (10) |
| $\alpha$ (°) | 90 | 90 |
| $\beta$ (°) | 92.927 (2) | 98.7540 (10) |
| $\gamma$ (°) | 90 | 90 |
| *V* (Å$^3$) | 5343.2 (5) | 4367.5 (3) |
| *Z* | 8 | 8 |
| $\rho_{calcd}$ (mg/m$^3$) | 1.510 | 1.920 |
| *F* (000) | 2336 | 2432 |
| Crystal size (mm) | 0.22 × 0.20 × 0.18 | 0.22 × 0.20 × 0.18 |
| Index ranges | $-24 \le h \le 34$ | $-9 \le h \le 11$ |
| | $-14 \le k \le 14$ | $-19 \le k \le 18$ |
| | $-18 \le l \le 17$ | $-35 \le l \le 32$ |
| $\theta$ range (°) | 1.31–25.22 | 1.40–25.19 |
| Final R indices [$I > 2\sigma$(I)] | $R_1 = 0.0420$ | $R_1 = 0.0639$ |
| | w$R_2 = 0.1312$ | w$R_2 = 0.1485$ |
| Data/restraints/parameters | 5059/101/328 | 7831/420/597 |
| Goodness-of-fit on $F^2$ | 1.067 | 1.383 |
| Largest diff. Peak/hole (eÅ$^{-3}$) | 3.043/−0.904 | 2.203/−3.098 |

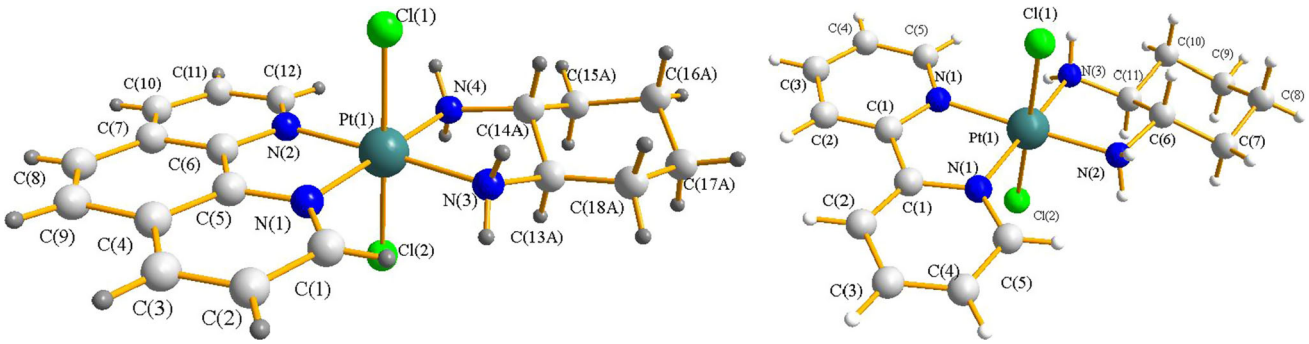


**Fig. 3** Crystal structures of (*left*) [Pt(phen)(*RR*-DACH)$Cl_2$]$Cl_2$ and (*right*) [Pt(bpy)(*SS*-DACH)$Cl_2$]$Cl_2$. The anions and one set of disordered atoms for the two Pt(IV) complexes are omitted for clarity

form of Ac-CPFC-$NH_2$ was characterized by ESI–MS in the positive mode $[M + H^+]^+$ *m/z* 508.17.

Reaction mechanisms for the oxidation of thiol-containing compounds by a series of Pt(IV) complexes have been studied using stopped-flow spectroscopy [20, 21, 23–25, 27, 28, 30–32], nuclear magnetic resonance spectroscopy [19], and mass spectroscopy [29]. Accordingly, a parallel mechanism, which included different protolytic species of thiol-containing compounds in reaction with the Pt(IV) complex, was proposed, and the reduction reaction was observed to occur through a halide-bridged activated complex. Taking all the above considerations into account, we believe that *trans*-$[PtCl_2(phen)(SS\text{-DACH})]^{2+}$ was reduced by GSH or Ac-CPFC-$NH_2$ through a halide-bridged activated complex mechanism.

## In vitro cytotoxicity

The cytotoxicities of the Pt(IV) complexes and their Pt(II) analogs, along with cisplatin as a reference, were tested

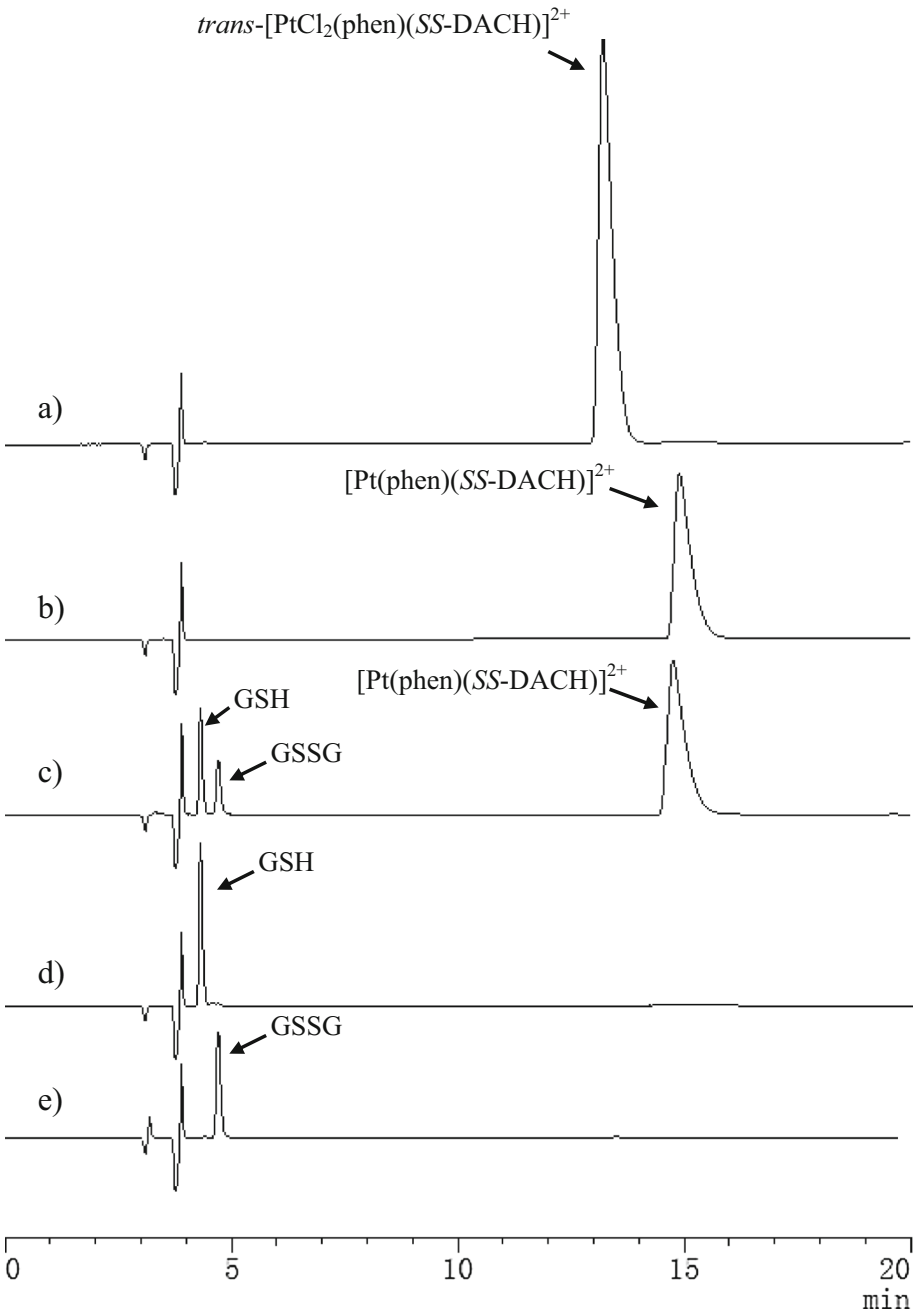


**Fig. 4** HPLC chromatograms of *a* 0.25 mM *trans*-$[PtCl_2(phen)(SS\text{-}DACH)]^{2+}$, *b* 0.25 mM $[Pt(phen)(SS\text{-}DACH)]^{2+}$, *c* the mixture of 0.25 mM *trans*-$[PtCl_2(phen)(SS\text{-}DACH)]^{2+}$ reaction with 0.75 mM GSH, *d* 0.75 mM GSH, and *e* 0.25 mM GSSG

against A549 and A549cisR cells. The $IC_{50}$ values are listed in Table 4. The cytotoxicities of the Pt(IV) complexes were almost the same as their corresponding Pt(II) complexes, which could reflect the reduction of the Pt(IV) complexes to their corresponding Pt(II) complexes in vivo [10]. All the tested platinum complexes were more cytotoxic than cisplatin, in both A549 and A549cisR cells. Moreover, all of the platinum complexes were more active against A549cisR cells than against A549 cells. For the four pairs of platinum complexes, the cytotoxicities of the (*SS*-DACH)-liganded platinum complexes were higher than those of the (*RR*-DACH)-liganded platinum complexes, in both A549 and A549cisR cells. Phen-liganded platinum complexes were more cytotoxic than were bpy-liganded platinum complexes. Moreover, the cytotoxicities of the four Pt(IV) complexes had no correlation with their reduction potentials.

## Conclusions

Four chiral DACH-liganded platinum(IV) complexes, containing intercalating ligands 1,10-phenanthroline and 2,2′-bipyridine, were synthesized successfully. The

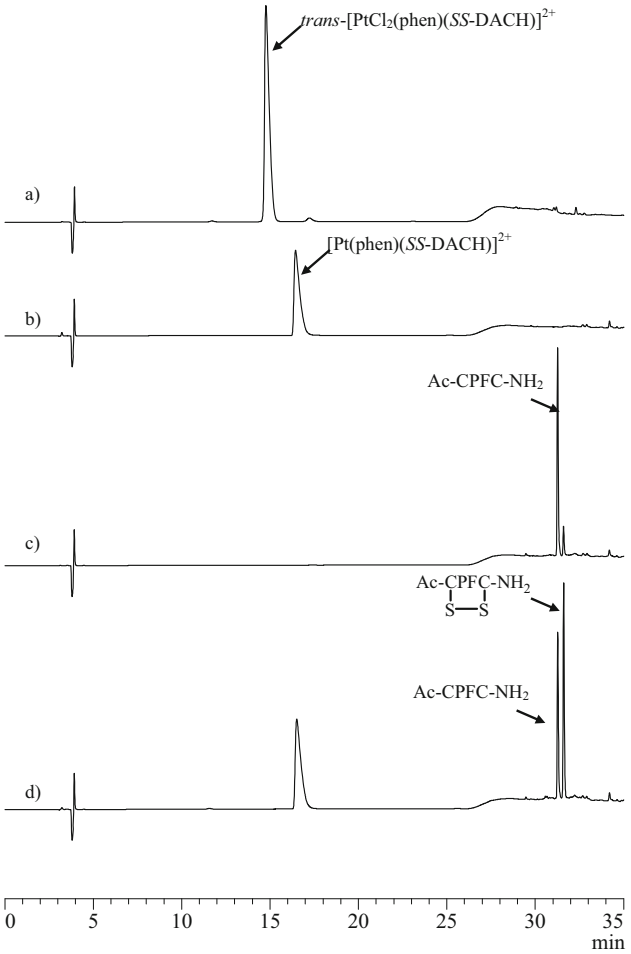


**Fig. 5** HPLC chromatograms of *a* 0.25 mM *trans*-$[PtCl_2(phen)(SS\text{-}DACH)]^{2+}$, *b* 0.25 mM $[Pt(phen)(SS\text{-}DACH)]^{2+}$, *c* 0.5 mM Ac-CPFC-$NH_2$, and *d* the mixture of 0.25 mM *trans*-$[PtCl_2(phen)(SS\text{-}DACH)]^{2+}$ reaction with 0.75 mM Ac-CPFC-$NH_2$

**Table 4** Cytotoxicities of different complexes in A549 and A549-cisR cells

| Compound | A549 | A549cisR |
|---|---|---|
| $[Pt(phen)(SS\text{-}DACH)Cl_2]Cl_2$ | 1.09 ± 0.05 | 0.22 ± 0.02 |
| $[Pt(phen)(RR\text{-}DACH)Cl_2]Cl_2$ | 2.57 ± 0.09 | 0.79 ± 0.02 |
| $[Pt(bpy)(SS\text{-}DACH)Cl_2]Cl_2$ | 14.5 ± 0.59 | 1.78 ± 0.16 |
| $[Pt(bpy)(RR\text{-}DACH)Cl_2]Cl_2$ | 24.9 ± 1.65 | 6.97 ± 0.67 |
| $[Pt(phen)(SS\text{-}DACH)]Cl_2$ | 1.13 ± 0.08 | 0.41 ± 0.01 |
| $[Pt(phen)(RR\text{-}DACH)]Cl_2$ | 2.37 ± 0.07 | 1.03 ± 0.02 |
| $[Pt(bpy)(SS\text{-}DACH)]Cl_2$ | 12.5 ± 0.64 | 1.36 ± 0.15 |
| $[Pt(bpy)(RR\text{-}DACH)]Cl_2$ | 4.2 ± 1.21 | 8.02 ± 0.66 |
| Cisplatin | 124 ± 16 | 222 ± 26 |

Cells were treated with the complexes for 48 h. Cytotoxicity data are presented as $IC_{50}$ in μM

complexes were characterized by various techniques. The X-ray crystal structures of $[Pt(phen)(RR\text{-}DACH)Cl_2]Cl_2$ and $[Pt(bpy)(SS\text{-}DACH)Cl_2]Cl_2$ revealed that the axial positions of the Pt(IV) complex were occupied by two chlorides. Cytotoxicity assays were performed against A549 and A549cisR cells. The four Pt(IV) complexes showed higher activity against A549 and A549cisR than did cisplatin. Moreover, the cytotoxicities of the Pt(IV) complexes were higher against A549cisR cells than against A549 cells. The cytotoxicities of the Pt(IV) complexes correlated with the type of intercalating ligand and ancillary ligand. The results of this study may help in the development of a new type of metallointercalator-based anticancer Pt(IV) complex.

**Acknowledgements** This work was supported financially by grants from the National Natural Science Foundation of China (21406047), the Natural Science Foundation of Hebei Province (B2016201014), and the Natural Science Foundation of Educational Commission of Hebei Province (ZD2016073), which are gratefully acknowledged.

## References

1. Boulikas T, Pantos A, Bellis E, Christofis P (2007) Cancer Ther 5:537–583
2. Zhang J, Liu D, Li Y, Sun J, Wang L, Zang A (2009) Mini-Rev Med Chem 9:1357–1366
3. Farrell NP (2011) Curr Top Med Chem 11:2623–2631
4. Kelland L (2007) Nat Rev Cancer 7:573–584
5. Wang D, Lippard SJ (2005) Nat Rev Drug Discov 4:307–320
6. Johnstone TC, Suntharalingam K, Lippard SJ (2016) Chem Rev 116:3436–3486
7. Quiroga AG (2011) Curr Top Med Chem 11:2613–2622
8. Chin CF, Wong DYQ, Jothibasu R, Ang WH (2011) Curr Top Med Chem 11:2602–2612
9. Hall MD, Mellor HR, Callaghan R, Hambley TW (2007) J Med Chem 50:3403–3411
10. Macias FJ, Deo KM, Pages BJ, Wormell P, Clegg JK, Zhang YJ, Li F, Zheng G, Sakoff J, Gilbert J, Aldrich-Wright JR (2015) Chem Eur J 21:16990–17001
11. Harper BW, Krause-Heuer AM, Grant MP, Manohar M, Garbutcheon-Singh KB, Aldrich-Wright JR (2010) Chem Eur J 16:7064–7077
12. Fisher DM, Fenton RR, Aldrich-Wright JR (2003) J Inorg Biochem 96:131
13. Garbutcheon-Singh KB, Leverett P, Myers S, Aldrich-Wright JR (2013) Dalton Trans 42:918–926
14. Fisher DM, Bednarski PJ, Grunert R, Turner P, Fenton RR, Aldrich-Wright JR (2007) ChemMedChem 2:488–495
15. Fisher DM, Fenton RR, Aldrich-Wright JR (2008) Chem Commun 43:5613–5615
16. Kemp S, Wheate NJ, Pisani MJ, Aldrich-Wright JR (2008) J Med Chem 51:2787–2794
17. Wilson JJ, Lippard SJ (2014) Chem Rev 114:4470–4495
18. Wexselblatt E, Gibson D (2012) J Inorg Biochem 11:7220–7229
19. Sinisi M, Intini FP, Natile G (2012) Inorg Chem 51:9694–9704
20. Lemma K, Shi T, Elding LI (2000) Inorg Chem 39:1728–1734
21. Lemma K, Berglund J, Elding LI (2000) J Biol Inorg Chem 5:300–306
22. Eastman A (1987) BioChem Pharmcol 36:4177–4178
23. Shi T, Berglund J, Elding LI (1996) Inorg Chem 34:3498–3503
24. Shi T, Berglund J, Elding LI (1997) J Chem Soc Dalton Trans 2073–2077

25. Lemma K, Sargeson AM, Elding LI (2000) J Chem Soc Dalton Trans 1167–1172
26. Nemirovski A, Kasherman Y, Tzaraf Y, Gibson D (2007) J Med Chem 50:5554–5556
27. Huo S, Shen S, Liu D, Shi T (2012) J Phys Chem B 116:6522–6528
28. Ren Y, Dong J, Shi H, Huo S, Dai T, Shi T (2015) Transit Met Chem 40:347–353
29. Liang B, Huo S, Ren Y, Sun S, Cao Z, Shen S (2015) Transit Met Chem 40:31–37
30. Huo S, Shen S, Liu D, Shi T (2014) Dalton Trans 43:15328–15336
31. Huo S, Dong J, Song C, Xu J, Shen S, Shi T (2014) RSC Adv 4:7402–7409
32. Huo S, Shi H, Liu D, Shen S, Zhang J, Song C, Shi T (2013) J Inorg Biochem 125:9–15
33. Sheldrick GM (2008) Acta Crystallogr A 64:112–122
34. Pages BJ, Zhang Y, Li F, Sakoff JG, Aldrich-Wright JR (2015) Eur J Inorg Chem 21:4167–4175
35. Guo S, Mason DN, Turland SA, Lawrenz ET, Kelly LC, Fallon GD, Gatehouse BM, Bond AM, Deacon GB, Battle AR, Hambley TW, Rainone S, Webster LK, Gullinace C (2012) J Inorg Biochem 115:226–239